

2 **Developing Integrated PBPK/PD Coupled mechanistic pathway**
3 **model (miRNA-BDNF): an approach towards System**
4 **toxicology**

4

5 Raju Prasad Sharma, Marta Schuhmacher, Vikas Kumar*

6

7

8

9*Center of Environmental Food and Toxicological Technology (TecnATox),*
10*Departament d'Enginyeria Química, Universitat Rovira i Virgili,*
11*Tarragona, Catalonia, Spain*

12

13

14

15

16

17

18* Corresponding author: Environmental Engineering Laboratory, Departament d'Enginyeria
19Química, Universitat Rovira i Virgili, Tarragona, Catalonia, Spain. Tel.: +34977558576.

20E-mail address: vikas.kumar@urv.cat

21

22

23**Abstract:**

24 Integration of a dynamic signal transduction pathway into the tissue dosimetry model is
25 a major advancement in the area of computational toxicology. This paper illustrates the
26 ways to incorporate the use of existing system biological model in the field of
27 toxicology via its coupling to the Physiological based Pharmacokinetics and
28 Pharmacodynamics (PBPK/PD) model. This expansion framework of integrated
29 PBPK/PD coupled mechanistic system pathway model can be called as system
30 toxicology that describes the kinetics of both -the chemicals and -biomolecules, help us
31 to understand the dynamic and steady-state behaviors of molecular pathways under
32 perturbed condition. The objective of this article is to illustrate a system toxicology
33 based approach by developing an integrated PBPK/PD coupled miRNA-BDNF pathway
34 model and to demonstrate its application by taking a case study of PFOS mediated
35 neurotoxicity. System dynamic involves miRNA-mediated BDNF regulation, which
36 plays an important role in the control of neuronal cell proliferation, differentiation, and
37 survivability.

38**Key words:** PBPK/PD, miRNA, BDNF, Neuroendocrine, System biology, PFOS

391. Introduction

40In the field of quantitative risk assessment, a journey of classical dose-response models
41is categorized into different classes for the better quantification and estimation of early
42possible risk (Andersen et al., 2005). These include –a) Physiological based
43pharmacokinetic and pharmacodynamic modeling (PBPK) for the quantification of
44internal biophase concentrations in different tissues, b) pharmacodynamics (PD) model
45quantifies the interactions of chemicals with target biomolecules c) System Biology
46describes the dynamic relationship of biological components for a robust physiological
47response. Perturbation of these biological components can be quantified through the
48integration of PBPK/PD model into the system biological models providing a predictive
49tool for measuring toxicological impact at the cellular and biomolecular level (Andersen
50et al., 2005; Gohlke et al., 2005; Zhao and Ricci, 2010).

51The PBPK model in the area of dosimetry risk assessment has been widely accepted and
52applied and it is among the top priority tool recommended in the vision of toxicity
53testing in the 21st century (Andersen and Krewski, 2009). PBPK model has been
54extended to develop the PBPK/PD for certain pesticides (Timchalk et al., 2002;
55Foxenberg et al., 2011). The integration of PD was generally done with the
56quantification of the response variable (biomarker) effect of an interaction of a chemical
57(biophase concentration estimated by PBPK) with a target biomolecule (mainly
58receptors). But it has a certain limitation such as lack of robust biology (biomarker
59relation to endpoint), and very often the endpoints are specifically remained single
60explanatory biomarker. Coupling of PBPK/PD model and system biology together can
61enlighten the effect of changes in key biomolecules considering the whole biological
62system. System biology comprising of genomics, metabolomics, and proteomics which
63rationalizes the functional interaction of biological components in a time-dependent
64fashion (Aderem, 2005; Kitano, 2002). Thus, it could be useful in system toxicology for
65understanding the altered biological pathway due to chemical induced perturbation of
66certain key biomolecule in a system, illustrating differences from normal pathway
67(Arrell and Terzic, 2010; Auffray et al., 2009; Hood et al., 2004; Kell, 2006).
68Understanding the biomolecular mechanisms are of great interest to identify the
69toxicological effects at the very early stages of the disease (toxicological response).
70However, often we lack sufficient information to link chemically perturbed biological
71components (molecular biomarker) to an altered biological system. This lead to the use
72of the simplified dose-response model (simple PD) to predict the adverse outcome
73(disease) for a target chemical(Calabrese and Baldwin, 2003). In the field of toxicology,
74there is limited use of these system biology models (Waters et al., 2003). The wide use
75of system toxicology in human environmental risk assessment has a time lag in
76comparison with pharmaceuticals science as it lacks experimental data, has complex
77interaction pathways of environmental chemicals than the target specific drugs, and low
78commercial priority of applied toxicological science.

79Recently use of the integrated PBPK/PD models in a field of environmental toxicology,
80enables development of a quantitative biologically based risk model which increases our
81understanding towards the relationship between tissue bio-phase concentration of
82chemicals and endogenous biomolecule (Timchalk et al., 2002; Foxenberg et al., 2011).
83Furthermore, signaling pathways could be used as an extension of PBPK/PD, given
84dynamic interactions of chemicals with biological components are known, the first step
85towards system toxicology (Bhattacharya et al., 2012; Gim et al., 2010). It has benefits
86such as: easy to implement if the signaling pathway already developed, often data from

87the dose-response experiments for known biomolecules can be used, a good step to use
88Adverse Outcome Pathways (AOPs) knowledge to develop the generic PBPK/PD
89model for multi-species and multi-chemicals.

90Neuroendocrine or neurotrophins such as nerve growth factors, BDNF and
91neurotrophin-3 are proteins, basically processed and secreted in constitutive and
92regulatory fashion in non-neuron, neurons and neuroendocrine cells (Lu, 2003; Mowla
93et al., 1999). Among them, BDNF is immensely expressed and extensively scattered
94than other neurotrophins, and play an important role in neuronal survival and
95differentiation (Boulle et al., 2012; Michael et al., 1997; Murer et al., 2001). BDNF
96binds with a Tropomyosin receptor kinase B (TrkB) presents on the neuronal cell
97surface causing sequential activation of following pathways such as Mitogen-activated
98protein kinases (MAPKs), Extracellular-signal-regulated kinase (ERK), and Protein
99kinase B (AKT) that are mainly involved in differentiation and survivability of neurons
100(Michael et al., 1997; Murer et al., 2001 Bursac et al., 2010; Boulle et al., 2012). It has
101been seen that reduced BDNF protein and mRNA expression is linked with several
102neurological disorders such as Alzheimer's and Parkinson's (Bursac et al., 2010).
103Moreover, dopaminergic, GABAergic, cholinergic, and serotonergic neurons are known
104to require BDNF for their proper development and survival (Lipsky and Marini, 2007;
105Murer et al., 2001), signifies BDNF as an important biomarker for neurodevelopmental
106function.

107It has been reported that miRNA regulates the synthesis of BDNF via
108posttranscriptional modification of BDNFmRNA (Caputo et al., 2011; You et al., 2016).
109Muiños-Gimeno et al., (2011) reported the involvement of miRNA-22 associated panic
110disorders in the Spanish and North European population. Later, the transcriptomic
111analysis studied by Li et al., (2015) in SH-SY5Y cell line also found the involvement of
112miRNA-22 dependent decrease in the BDNF level and neuronal cell survivability. The
113miRNAs are turning out to be significant regulators of mRNAs and the related proteins.
114In this proposed study, miRNA (micro-RNA) regulated BDNF (Brain- derived
115neurotropic factor) and its effect on neuronal survivability mechanisms was selected for
116the development of the mechanistic base model. Perfluorooctanesulfonic acid (PFOS)
117was selected as a case study to illustrate the ways to incorporate the use of system
118biological model in the field of toxicology via Pharmacodynamic coupled tissue
119dosimetry model(PBPK/PD).

120Case studies on PFOS

121PFOS is well recognized among industrial chemicals that can easily cross the BBB
122(blood brain barrier) (Sato et al., 2009) and its exposure was related to several
123developmental neurotoxicity effects (Johansson et al., 2008; Yang et al., 2015; Goudarzi
124et al., 2016; Vuong et al., 2016) . For instance, it was found that PFOS exposure to
125zebrafish causing an alteration in the expression of more than 40 different type of
126miRNAs allied with the developmental toxicities (Zhang et al., 2011). The several
127mechanisms were hypothesized for the PFOS causing development neurotoxicity
128disorders such as oxidative stress, altering neurotransmitters level and upregulation and
129downregulation of apoptotic and pro-survival factors from various animals and cell line
130studies (Long et al., 2013; Chen et al., 2014; Yu et al., 2016). In a recent study, it was
131found that PFOS can decrease the neuronal cell survivability by altering the level of
132miRNA in human neuroblastoma cell line(Li et al., 2015). This could be an important
133mechanism of PFOS as it has been seen that miRNAs regulate the proteins level by

134regulating their mRNAs expression level. The purpose of our model is to test the
135hypothesis that PFOS perturbed the miRNA affecting neuronal survivability via
136regulating BDNF at mRNA level. The human dosimetry study has shown the longer
137residence time of PFOS inside the body and relatively higher concentration in the brain
138tissue than comparing to other perfluoroalkyl substances (PFASs) (Fabrega et al., 2014).
139Furthermore, its continuous exposure and potential to cross the BBB could put the
140humans at high risk of neurodevelopmental disorders which is in consonance with
141recently published paper related to neurotoxicity of PFOS (Yang et al., 2015; Vuong et
142al., 2016). The PFOS PBPK model has been well developed previously by Fabrega et
143al., (2014) that predicts internal tissue dose. However, for a better understanding of
144toxicological mechanisms in the context of risk assessment, we would need one more
145step towards the system toxicology. This gap could fill by coupling integrated
146PBPK/PD model into a mechanistic system model.

147The objective of this study was the development of a mechanistic pathway system
148(miRNA-BDNF mRNA- BDNF- cell survivability) model and coupling of above model
149with a PBPK/PD taking a case study of the PFOS induced neurotoxicity.

150

151**2. Materials and Methods**

152**2.1. miRNA-mRNA-BDNF-cell survival mechanistic pathway (figure 1)**

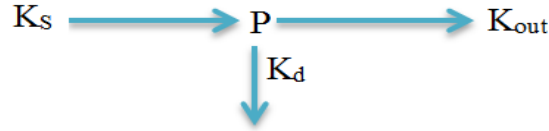
153Generally, miRNA post-transcriptionally regulates the protein molecule via binding at 3
154'UTR of mRNA (Perruisseau-Carrier et al., 2011). It has been found that miRNA
155decreases the level of BDNF either via degradation of mRNA or facilitating ribosome
156induced silencing complex formation with mRNA (RISCm) (Bartel, 2004; Djuranovic
157et al., 2011). The other mechanism involves miRNA inhibits the BDNF regulation by
158downregulating the expression of cyclic response element-binding protein (CREB)
159(Caputo et al., 2011; You et al., 2016). Nonetheless, the numbers of the regulatory
160pathways have been proposed (Zeng et al., 2011; Sandhya et al., 2013; York, 2015).
161Moreover, a study on population affected with neuronal disorders showed an inverse
162relationship between miRNA and BDNF level (Muiños-Gimeno et al., 2011)
163strengthens the evidence of regulation of BDNF via miRNA. BDNF dependent cell
164survival pathways can be extremely important from a regulatory perspective. The
165relationship between BDNF concentration and cell survival are quite well known via the
166dose-response curve obtained from the in-vitro cell line study (O'Leary and Hughes,
1671998). Nevertheless, intermediate molecular signaling pathways are prevailed in-
168between the binding of BDNF with TrkB receptors to the effects on the neuronal cell.
169This involves activation of MAPK/ERK and AKT-PI3K pathways that increase the
170neuronal survival and differentiation process via increasing expression of CREB
171(Michael et al., 1997; Murer et al., 2001 Bursac et al., 2010; Boulle et al., 2012). The
172conceptual diagram is provided in figure 1.

173**2.1.1. miRNA regulatory BDNF pathway model**

174The regulatory pathway of BDNF involves different intermediate biomolecules.
175However, in this study, the generic miRNA-BDNF pathway was adapted from the
176previously published work of Wang et al., (2010) to developed exclusively miRNA
177regulatory BDNF model. The whole pathways are modeled by applying mass balance
178equation based on reaction kinetics applying ordinary differential equations. This
179allows the estimation of a biomolecule given the model parameter corresponds to the

180reaction rates. BDNF is the output of the miRNA-BDNF model, which was then used as
 181an input for the estimation of neuronal survival. The generic form of the system
 182dynamic model is as follow:

183



184

185Where K_s is synthesis rate constant for the endogenous molecules, P is the
 186concentration of an endogenous molecule, K_d is the degradation rate constant, K_{out} is
 187the dissipation rate constant of P available for the synthesis of the subsequent
 188endogenous molecule. Following this schematic, concentration of endogenous
 189biomolecules is estimated by the following differential equation;

190
$$\frac{d}{dt}(P) = K_s - K_d * P - K_{out} * P \quad \text{Eq. (1)}$$

191

1922.1.2. BDNF - cell survival Emax model-

193To simplify the model, we have applied hills sigmoid equations to get the output of the
 194neuronal survival by applying E_{max} and EC_{50} value of BDNF for neuronal cell
 195survival from experimental data (O’Leary and Hughes, 1998). The percentage of cell
 196survivability with respect to BDNF concentration was estimated by the use of sigmoid
 197Emax model applying the following equations;

198
$$Cell\ survivability = E_0 + \frac{E_{max} * C^n}{EC_{50} + C^n} \quad \text{Eq. (2)}$$

199Where, $Cell\ survivability$ = percentage of cell survivability as function of BDNF
 200conc., E_0 = baseline response, E_{max} = maximum response, C = BDNF concentration,
 201 EC_{50} = concentration at which BDNF shows 50% response of E_{max} , n = hill coefficient

202This developed Emax model was integrated into indirect response model eq. (3) that
 203provides the neuronal cell survivability as a function of time. More details on indirect
 204response models can be found in Bonate, (2011).

205
$$\frac{d}{dt} Cell\ survivability = k_{out_{BDNF}} * cell\ survivability - kd * cell\ survivability(t) \quad \text{Eq. (3)}$$

206

207Where $\frac{d}{dt} Cell\ survivability$ = percentage of cell survivability \in the time domain ,
 208 $k_{out_{BDNF}}$ is BDNF conc. assumed to be responsible for neuronal cell survivability,
 209 kd is the degradation rate of the neuronal cell.

2102.2. PFOS PBPK (a case study)

211The PBPK model of PFOS was adapted from the previously published model (Fabrega
 212et al., 2014). The concentration of PFOS in a brain considered as the effective target
 213dose (target tissue dosimetry), considering the brain as a target organ in relation to
 214potential neurodevelopment deficit disorders. PBPK model generates time course of
 215PFOS concentration in the brain, which is used as input for the mechanistic pathway
 216model. At the end, integration of the PBPK model of PFOS into the mechanistic BDNF
 217–cell survivability model analyzes the perturbation of PFOS on the whole pathway
 218results in decreased in neuronal cell survival rate. The conceptual model for this
 219integration is provided in figure 2.

220Concentrations in the respective compartment (muscle, richly perfused, fat, kidney,
 221Brain and liver) are estimated by applying the following equation:

222

$$223 \frac{dC_i}{dt} = \frac{Q_i \times \left(C_a - \frac{C_i}{K_i:p} \right)}{V_i} \quad \text{Eq. (4)}$$

225Where, C_i is the concentration in the tissue i (ng/L), Q_i is the blood flow in the tissue i
 226(L/h), C_a is the arterial concentration (ng/L), $K_i:p$ is the partition coefficient of tissue i ,
 227and V_i is the volume of the tissue i (L). Detail description of PBPK model can be found
 228in our other publications (Fabrega et al., 2014; Fàbrega et al., 2016).

229All the physiological, Physicochemical parameters and model equations for the PBPK
 230are provided in the Annex-I

2312.3. IVIVE for dose Equivalency

232In-vitro in-vivo extrapolation (IVIVE) method was used in order to estimate the oral
 233equivalent dose from the given in-vitro dose. It has an assumption that the in-vitro area
 234under the curve (AUC), calculated by multiplying dose with the total duration of
 235exposure, would be similar with the AUC of target in-vivo organ (in this case Brain).

236Li et al., (2015) in-vitro studies on SH-SY5Y cell line was selected, where a decrease in
 237neuronal cell survivability found to depend on miRNA and BDNF. In Li et al., an
 238experiment they used 12 in-vitro doses (6 doses each for 24hr and 48 hr) for that
 239corresponding in vivo doses was determined. The assumption was made that in-vitro
 240doses are equivalent to internal target concentration (brain). For the reconstructing
 241equivalent oral dose, the AUC value was calculated for each in-vitro conc., based on
 242their duration of treatment (In this case 24hr and 48 hr). The conceptual schematic for
 243dose reconstruction is provided in figure 3. The calculated AUC was assumed to be
 244equivalent with in-vivo AUC brain. Dose reconstruction approach has been used, so that
 245the given equivalent oral dose will provide the AUC in the brain that matches the AUC
 246for the 12 different in-vitro doses (6 for 24hr and 6 for 48hr), a similar approach has
 247been used in the previous study (Thiel et al., 2017). The oral equivalent doses were
 248estimated to be way higher, as the PFOS concentration reaching to the brain was found
 249to be relatively very low(Fabrega et al., 2014; Fàbrega et al., 2016). The estimated oral
 250equivalent doses for the corresponding in-vitro doses are provided in Table 1.

2512.4. Integrated PBPK/PD coupled miRNA-BDNF-cell survival pathway

252 Coupling of PBPK to mechanistic miRNA-BDNF pathway model has been done with
 253 the integration of brain PFOS concentration as a target input that perturbs key
 254 component miRNA of the pathway. The interaction of the PFOS with the miRNA has
 255 been done based on empirical evidence but the mechanism behind the interaction is still not
 256 clear. The coupling was done by applying stimulatory Emax model that assumes PFOS
 257 increase the concentration of miRNA via increasing their synthesis rate. Finally the
 258 output we measured as a percentage of neuronal survival rate considering two scenarios;
 259 with and without PFOS exposure. The conceptual diagram is provided in figure 4.

260 The integration of PFOS into the BDNF pathway is done by indirect pharmacodynamic
 261 interaction model with the following equation;

$$262 \quad \frac{d}{dt}(miRNA) = K_{i miRNA} * \left(1 + \frac{Emax * C}{E C_{50} + C} \right) - K_{out miRNA} * miRNA \quad A_0 \quad \text{Eq. (5)}$$

263 Where, $K_{i miRNA}$ = synthesis rate constant of miRNA, $K_{out miRNA}$ = dissipation rate
 264 of miRNA, $miRNA_0$ = initial value of miRNA, Emax = maximum response for
 265 miRNA, C = brain concentration of PFOS, EC50 = concentration at which PFOS shows
 266 50% response of Emax.

267

268 2.5 Model parameterization

269 The mi-RNA-mRNA-Protein pathway parameters were taken from the previously
 270 published model (Wang et al., 2010). Specifically, BDNF protein synthesis rate was
 271 used instead of generic protein synthesis. There was no BDNF mRNA synthesis rate
 272 data available in the literature and for that generic BDNF mRNA rate constant was used.
 273 BDNF synthesis rate was taken from the Castillo et al., (1994) and Menei et al., (1998).
 274 Furthermore, the synthesis rate was scaled accounting number of neuronal cells to the
 275 whole body per kg weight nmol/hr/kg^(0.75). The degradation rate of BDNF was
 276 parameterized from half- life by using the following relationship: degradation rate =
 277 $\ln 2 / t_{1/2}$.

278 For the quantification of neuronal survival against BDNF exposure, the required Emax
 279 and EC50 parameters for establishing sigmoid Emax model were taken from O'Leary
 280 and Hughes, (1998). The Emax and EC50 values for the reaction are implemented as
 281 such as these parameters tend to have a similar trend across species (Gatzeva-topalova
 282 et al., 2011). PBPK parameters for the PFOS were used from the previously published
 283 article (Fabrega et al., 2014). The dynamic interaction data for the PFOS to miRNA,
 284 such as EC50 estimated from Li et al., (2015). All the parameters that were used for
 285 developing mechanistic model are provided in Table 2. All the model equations for the
 286 mechanistic and integrated PBPK/PD-mechanistic models are provided in the Annex-I

287

288 3. Results

289 The simulation of the model is divided into two parts; the first simulation of a PBPK
 290 and a mechanistic system pathway model individually to get the base model. Later
 291 simulation of integrated PBPK/PD coupled mechanistic model (system toxicology) was
 292 done. The integration of Pharmacodynamic interaction between PFOS and target

293biomolecule was done by using indirect response model. The equivalent exposure doses
294for the PFOS were extrapolated from the in-vitro study of Li et al., (2015). Neuronal
295survivability was chosen as an end point biomarker for the model and mapping of in-
296vitro data (neuronal survivability) to in-vivo was done based on linear interpolation
297method. The PFOS PBPK model codes are provided by Fabrega et al., (2014) which
298was used in this paper to simulate PBPK model.

299The mechanistic system model simulations were performed for the miRNA-BDNF
300signaling pathway and the resulting time course of BDNF was recorded as model
301output. The output of the BDNF time course data was used for performing the
302simulation to get the percentage of cell survivability by applying indirect sigmoid
303response model. This part of simulation results recorded as the normal baseline value
304for the model. The figure 6 (base model of the mechanistic pathway) showed the
305baseline value of important endogenous biomolecules like miRNA, BDNF, RISC(RNA-
306induced silencing complex), RISCm (complex form between BDNFmRNA and RISC)
307and percentage of neuronal cell survivability. The mechanistic system model has
308optimized to achieve the maximum neuronal cell survivability steady state which is in
309compliance with experiment data given by Gillespie et al., (2003). The model has been
310simulated for 20 days in order to achieve the steady state. The miRNA regulation of
311BDNF via forming a complex between RISC and BDNFmRNA called RISCm has been
312documented can be seen in the base model figure number 6 which is in compliance with
313Wang et al., (2010) model. This complex formation between RISC and BDNFmRNA
314was enhanced by the miRNA resulting in a decrease of BDNF protein synthesis. The
315RISC complex binds with the mRNA at the 3' UTR and inhibits its further translation to
316protein. The base model also able to capture the phenomena of regulating BDNF protein
317by miRNA considered to be one of the important biological processes. The behavior of
318model curve for BDNF and cell survival are in a similar trend, which was also observed
319in in-vivo experiments (Rodríguez-Tébar et al., 1992; O'Leary and Hughes, 1998;
320Fletcher et al., 2008). The model shows BDNF maintains cell survivability at the steady
321state level of around 95 percent. In Figure (6), a sudden drop in the cell survivability to
32240 percent level could be explained considering the lag time in the attainment of BDNF
323steady state level. The simulation of the base model (Figure 6) shows that model able to
324retain the steady state for cell survivability at 95% once BDNF attained a steady state.
325A similar observation was reported by Gillespie et al., (2003) experimental study that
326survivability of neuron in presence and absence of BDNF were 90 percent and 40
327percent respectively.

328The PBPK model simulation was carried out for the PFOS for the estimated oral
329equivalent dose (12 doses) given as a single dose. Figure 5 shows the simulation of the
330internal target tissue (brain) concentration of PFOS with 12 different dose levels
331providing different Cmax in dose dependent manner over the time period. The dose was
332given at the 240hr as shown in figure 6 when the mechanistic base model reaches steady
333state.

334The coupling of PBPK into the mechanistic model was done by fitting in-vitro data,
335estimated from Li et al., (2015) study, via applying Emax sigmoid model. The
336developed coupled PBPK/PD-mechanistic model quantifies the dynamic of the
337endogenous biomolecular concentration of different species at the different level of
338PFOS exposure that perturb key components of the system (in the miRNA model). The
339interaction of the PFOS to the given pathway was modeled by implementing indirect
340sigmoid response model **Eq. (5)** for PFOS-miRNA interaction. Consequently, dynamic

341changes in miRNA level as a function of PFOS concentration over time was observed
342(figure 7). The PFOS alter the steady state of all biological components involved in the
343pathway via stimulating input of miRNA disturbing whole mechanistic pathway. The
344integrated model was simulated for 12 different in-vitro equivalent in-vivo doses
345describing the whole system as one unit rendering time course of endogenous
346concentration after exposure to environment chemicals distinct from normal condition
347(Base model).

348The figure 7, 8, 9 and 10 shows the effect of a chemical on the endogenous biomolecule
349concentration (miRNA, RISCm, BDNF) and cell survivability (in percentage)
350respectively over the time period. Figure 7 illustrates the dose depended effects of
351PFOS on miRNA level following single exposure to PFOS (dose given at 240hr).
352Figure 8 illustrates the increase in the formation of the RISCm complex after the PFOS
353exposure. The increase of RISCm complex concentration is due to increase of miRNA
354level which can be considered as an indirect action of PFOS. The highest level of
355miRNA is observed at t_{max} (time point of C_{max}) of PFOS and, with the elimination of
356PFOS from the system, shifting of miRNA level to steady state concentration at the
357level higher than baseline concentration was observed. Consequently, a decrease in the
358level of BDNF (figure 9) was noted as increase miRNA level facilitates the formation of
359the RISCm (figure 8), posttranscriptional regulatory mechanism of miRNA (explained
360in 2.1). With the increase in dose level, the difference between base steady state
361concentration and shifted steady state concentration was higher that can be seen in
362figure 7, 8, 9 and 10. Figure 10, illustrates the time vs neuronal survivability that
363describes the effect of PFOS over time as an end point biomarker.

364**5. Discussion and Conclusions**

365In this study, an attempt was made for the development of an integrated PBPK/PD
366coupled mechanistic model that allows assessing or characterizing the potential impact
367of environmental chemicals on a biological system. An Integrated PBPK/PD PFOS
368model and a mechanistic (miRNA-BDNF-neuronal survival) system model were
369evaluated individually. The generic mi-RNA model was adapted with a modification in
370BDNF as a target output protein. The regulation of BDNF involves several pathways
371among which miRNA-dependent pathway is an important one. The endogenous level of
372BDNF has an important effect on the survivability of neurons. For example principal
373hierarchy of BDNF signaling and consequently activation of MAPK/ERK/AKT
374pathway is well understood (Michael et al., 1997; Murer et al., 2001 Bursac et al., 2010;
375Boulle et al., 2012), but how these events control cellular survival are not well
376understood. The reported relation between chemical exposure and significant changes in
377BDNF level, consequently neuronal adverse outcomes, made a plausible argument of
378considering BDNF as a good biomarker. To keep biological plausibility intact in our
379mathematical expression, we restrict our model to the miRNA-BDNF pathway, and
380later linking it to the cell survivability as a function of the time course of BDNF
381concentration by applying Emax model. The developed mechanistic model shows
382miRNA-dependent regulation of BDNF which is a natural phenomenon of this model
383retaining the regulatory mechanism of miRNA on BDNF. The mechanistic base model
384(figure 6) well predicted the percentage of cell survivability as a function of BDNF
385concentration. The PBPK model was used to estimate the internal target dose of
386chemicals. The output of PBPK in target organ is used as input for the mechanistic
387system model providing integrated coupled PBPK/PD-mechanistic system model. This
388will describe the whole system as one unit rendering time course of endogenous

389biomolecules concentration and their steady state level with and without chemical
390exposure marking the difference between the normal and altered biology of the
391pathway.

392The integrated PBPK/PD- coupled mechanistic system model well describes the
393observed changes in endogenous molecules level during and after discontinuation of
394exposure to the chemical. It can predict the adverse effect of environment chemicals
395considering both; the nature of changes in the system (altered biology) with respect to
396normal biology, and, the capability of an endogenous molecule to retain homeostasis,
397mimicking the real in vivo physiological scenario. Therefore, this kind of model
398(integrated PBPK/PD- coupled mechanistic system model) can predict risk in more
399quantitatively as well as mechanistically considering pharmacokinetic,
400pharmacodynamic and relative altered biology from normal biology pathway as a
401consequence of chemical exposure. The advantage of Coupled integrated PBPK/PD-
402mechanistic system model is; it provides more understanding towards risk not only
403based on the target tissue concentration but also their effect on the target molecule
404participating in the biological network. Integrated PBPK/PD coupled mechanistic model
405are able to predict endogenous molecule concentration involved in pathway over their
406time course as a function of chemical exposure, which was shown by current developed
407model as a case study for PFOS

408In summary, a molecular/cellular model that presented in this article mechanistically
409links BDNF involved in directed neuronal growth and neuronal survival, two distinct
410neurodevelopmental processes that use an overlapping molecular (that is genetic)
411machinery. The model does not provide further insights into which of these
412neurodevelopmental processes would be most relevant to the etiology of neurotoxicity,
413or where in the brain these processes are localized to selectively impact on neural
414circuitry. Although epigenetically regulation of BDNF (Lubin et al., 2008) in the brain
415by miRNA is very important were observed from literature in the theoretical network, it
416is unlikely that there would just be a single explanatory model that connects to BDNF
417on a molecular level and corresponding neuronal adverse outcomes. Rather, several
418etiologically cascades contributing to neuronal adverse outcome are likely to exist.
419However, the currently developed model considered the following pathway for a series
420of signaling cascade biomolecules such as chemicals-miRNA-mRNA-RISCm-BDNF-
421neuronal survivability, previously described in the conceptual model (figure 2). For the
422currently selected pathway model predicts BDNF as a very sensitive endogenous
423species biomolecule, which maintains the cell survivability at steady state. Although,
424PFOS does not directly target BDNF in our model it still remains the sensitive target
425which could be due to its regulation is highly dependent on miRNA level. Comparison
426of figure 9 and 10 allow us to see the decrease in neuronal survivability (figure 10) is
427highly sensitive towards BDNF level (figure 9). The model shows that BDNF regulation
428(miRNA based regulation) is very much important for neuronal cell survivability. This
429shows BDNF could be an interesting species (biomarker) which can link between both
430environmental exposure and neuronal adverse outcomes.

431There was an assumption of the existence of an empirical relation between the in-vitro
432toxicity to in-vivo toxicity (Wambaugh et al., 2013). Moreover, tools have been
433developed to translate in-vitro toxicity dose-response to predict the in-vivo toxicity by
434applying reverse dosimetry concept that provides equivalent in-vivo dose required to
435produce in-vitro toxicity, eventually validation of model was done by comparing POD
436(point of departure) from predicted in vivo dose response with reported POD of

437chemicals (Abdullah et al., 2016; Forsby and Blaauboer, 2007; Louisse et al., 2016;
438Wambaugh et al., 2013). In this case study of PFOS model (PBPK/PD coupled
439mechanistic model) due to lack of in-vivo data particularly for the following proposed
440mechanistic pathway, in worst case scenario we constrained to in-vitro data for
441qualitative or partial validation of the developed model. To check the performance of
442the developed PBPK/PD coupled mechanistic model, neuronal cell survivability was
443selected as an end point. Two approaches were used for this purpose; first
444reconstructing oral in-vivo equivalent dose for an in-vitro dose; second, response data
445are generated for identified in vivo doses by mapping in vitro toxicity data (in this case
446neuronal cell survivability). Figure 10 illustrates, the simulated response variable (%
447neuronal survivability), for dose equivalent to in-vitro conc., vs observed linear
448interpolated response variable. Although model could not able to predict all the
449observed data, however, most of them were within the simulated range. The simulated
450maximum % of neuronal cell survivability on the lower side was around 35%, which is
451higher than the experimental observation of around 16 to 20%. This could be possibly
452explained by several facts such as current model uses adaptability mechanism which
453lacks in the in-vitro system, only one pathway has been accounted, neglecting the
454possibility of several mechanisms, empirical estimation of PFOS-miRNA interaction
455and the inherent uncertainty in in-vitro data and model.

456The purpose of this work was to develop a simple model which combines
457pharmacokinetic model like PBPK predicting the internal tissue dosimetry and
458mechanistic system model via quantifying the Pharmacodynamic interaction of
459chemicals with key biomolecule components involved in the mechanistic system of
460biology. The measurement of mi-RNA, mRNA, BDNF in the brain at different time
461points gives evidence in parallel changes and difference in between them; significantly
462improves the understanding of relation with neuronal adverse outcomes. Here in this
463model, the mechanistic pathway can be considered as an equivalent AOP pathway for
464neurotoxicity. However, this can be further extended by integrating identified new
465pathways responsible for neurotoxicity. There are many ways that model can be
466extended to increase its utility, but certainly, the mi-RNA-based post-transcription
467regulation of BDNF not limited to PFOS. The same concept can be further applied to
468other environmental chemicals altering the similar system.

469In this paper, we have partially validated our model, considering our objective of this
470paper is to focus on the illustration of tools that use simple integrated PBPK/PD-
471coupled mechanistic pathway model involving three main steps 1. Development of
472PBPK model, 2. Development of mechanistic system model 3. Couple PBPK with the
473mechanistic model by integrating PD model that quantify perturbed biomolecule (a
474component of the mechanistic model) as a result of chemical exposure. This step
475developed a new framework that could utilize the existing normal mechanistic pathways
476model and integrated PBPK/PD model, a step towards system toxicology based models.

477**Acknowledgement**

478Preparation of this manuscript was supported in part for European Union's projects,
479HEALS (Health and Environment-wide Associations via Large population Surveys) by
480the FP7 Programme under grant agreement no. [603946](#) and EuroMix (European Test
481and Risk Assessment Strategies for Mixtures) by the Horizon 2020 Framework
482Programme under grant agreement no. [633172](#). Raju Prasad Sharma has received a
483doctoral fellowship from Universitat Rovira i Virgili under Martí-Franquès Research

484Grants Programme. This publication reflects only the authors' views. The Community
485and other funding organizations are not liable for any use made of the information
486contained therein.

487References

- 488Abdullah, R., Alhusainy, W., Woutersen, J., Rietjens, I.M.C.M., Punt, A., 2016.
489 Predicting points of departure for risk assessment based on in vitro cytotoxicity
490 data and physiologically based kinetic (PBK) modeling: The case of kidney
491 toxicity induced by aristolochic acid I. *Food Chem. Toxicol.* 92, 104–116.
492 doi:10.1016/j.fct.2016.03.017
- 493Aderem, A., 2005. Systems biology: Its practice and challenges. *Cell* 121, 511–513.
494 doi:10.1016/j.cell.2005.04.020
- 495Andersen, M.E., Krewski, D., 2009. Toxicity testing in the 21st century: Bringing the
496 vision to life. *Toxicol. Sci.* 107, 324–330. doi:10.1093/toxsci/kfn255
- 497Andersen, M.E., Thomas, R.S., Gaido, K.W., Conolly, R.B., 2005. Dose-response
498 modeling in reproductive toxicology in the systems biology era. *Reprod. Toxicol.*
499 19, 327–337. doi:10.1016/j.reprotox.2004.12.004
- 500Arrell, D.K., Terzic, a, 2010. Network systems biology for drug discovery. *Clin.*
501 *Pharmacol. Ther.* 88, 120–125. doi:10.1038/clpt.2010.91
- 502Auffray, C., Chen, Z., Hood, L., 2009. Systems medicine: the future of medical
503 genomics and healthcare. *Genome Med.* 1, 2. doi:10.1186/gm2
- 504Bartel, D.P., 2004. MicroRNAs: Genomics, Biogenesis, Mechanism, and Function. *Cell*
505 116, 281–297. doi:10.1016/S0092-8674(04)00045-5
- 506Bartlett, D.W., Davis, M.E., 2006. Insights into the kinetics of siRNA-mediated gene
507 silencing from live-cell and live-animal bioluminescent imaging. *Nucleic Acids*
508 *Res.* 34, 322–333. doi:10.1093/nar/gkj439
- 509Bhattacharya, S., Shoda, L.K.M., Zhang, Q., Woods, C.G., Howell, B.A., Siler, S.Q.,
510 Woodhead, J.L., Yang, Y., McMullen, P., Watkins, P.B., Melvin, E.A., 2012.
511 Modeling drug- and chemical-induced hepatotoxicity with systems biology
512 approaches. *Front. Physiol.* 3 DEC, 1–18. doi:10.3389/fphys.2012.00462
- 513Bonate, P.L., 2011. *Pharmacokinetic-Pharmacodynamic Modeling and Simulation.*
514 Springer US, Boston, MA. doi:10.1007/978-1-4419-9485-1
- 515Boulle, F., van den Hove, D.L. a, Jakob, S.B., Rutten, B.P., Hamon, M., van Os, J.,
516 Lesch, K.-P., Lanfumey, L., Steinbusch, H.W., Kenis, G., Hove, D.L.A. Van Den,
517 Jakob, S.B., Rutten, B.P., Hamon, M., Os, J. Van, Lesch, K.-P., van den Hove,
518 D.L. a, Jakob, S.B., Rutten, B.P., Hamon, M., van Os, J., Lesch, K.-P., Lanfumey,
519 L., Steinbusch, H.W., Kenis, G., 2012. Epigenetic regulation of the BDNF gene:
520 implications for psychiatric disorders. *Mol. Psychiatry* 17, 584–596.
521 doi:10.1038/mp.2011.107
- 522Bursac, N., Kirkton, R.D., Mcspadden, L.C., Liao, B., 2010. Circulating levels of brain-
523 derived neurotrophic factor: correlation with mood, cognition and motor function.
524 *Biomark. Med.* 4, 871–87.

- 525 Calabrese, E.J., Baldwin, L.A., 2003. Toxicology rethinks its central belief. *Nature* 421,
526 691–692. doi:10.1038/421691a
- 527 Caputo, V., Sinibaldi, L., Fiorentino, A., Parisi, C., Catalanotto, C., Pasini, A., Cogoni,
528 C., Pizzuti, A., 2011. Brain derived neurotrophic factor (BDNF) expression is
529 regulated by microRNAs miR-26a and miR-26b allele-specific binding. *PLoS One*
530 6. doi:10.1371/journal.pone.0028656
- 531 Carlotti, F., Dower, S.K., Qwarnstrom, E.E., 2000. Dynamic shuttling of nuclear
532 factor τ B between the nucleus and cytoplasm as a consequence of inhibitor
533 dissociation. *J. Biol. Chem.* 275, 41028–41034. doi:10.1074/jbc.M006179200
- 534 Castillo, B., del Cerro, M., Breakefield, X.O., Frim, D.M., Barnstable, C.J., Dean, D.O.,
535 Bohn, M.C., 1994. Retinal ganglion cell survival is promoted by genetically
536 modified astrocytes designed to secrete brain-derived neurotrophic factor (BDNF).
537 *Brain Res.* 647, 30–36. doi:10.1016/0006-8993(94)91395-1
- 538 Chen, N., Li, J., Li, D., Yang, Y., He, D., 2014. Chronic exposure to perfluorooctane
539 sulfonate induces behavior defects and neurotoxicity through oxidative damages, in
540 Vivo and in Vitro. *PLoS One* 9, 1–10. doi:10.1371/journal.pone.0113453
- 541 Clarke, G., Collins, R.A., Leavitt, B.R., Andrews, D.F., Hayden, M.R., Lumsden, C.J.,
542 McInnes, R.R., 2000. A one-hit model of cell death in inherited neuronal
543 degenerations. *Nature* 406, 195–199. doi:10.1038/35018098
- 544 Djuranovic, S., Nahvi, A., Green, R., 2011. A Parsimonious Model for Gene Regulation
545 by miRNAs. *Science* (80-.). 331, 550–553. doi:10.1126/science.1191138
- 546 Fabrega, F., Kumar, V., Schuhmacher, M., Domingo, J.L., Nadal, M., 2014. PBPK
547 modeling for PFOS and PFOA: Validation with human experimental data. *Toxicol.*
548 *Lett.* 230, 244–251. doi:10.1016/j.toxlet.2014.01.007
- 549 Fabrega, F., Nadal, M., Schuhmacher, M., Domingo, J.L., Kumar, V., 2016. Influence
550 of the uncertainty in the validation of PBPK models: A case-study for PFOS and
551 PFOA. *Regul. Toxicol. Pharmacol.* 77, 230–239. doi:10.1016/j.yrtph.2016.03.009
- 552 Fletcher, J.M., Morton, C.J., Zwar, R.A., Murray, S.S., O’Leary, P.D., Hughes, R.A.,
553 2008. Design of a conformationally defined and proteolytically stable circular
554 mimetic of brain-derived neurotrophic factor. *J. Biol. Chem.* 283, 33375–33383.
555 doi:10.1074/jbc.M802789200
- 556 Forsby, A., Blaauboer, B., 2007. Integration of in vitro neurotoxicity data with
557 biokinetic modelling for the estimation of in vivo neurotoxicity. *Hum. Exp.*
558 *Toxicol.* 26, 333–338. doi:10.1177/0960327106072994
- 559 Foxenberg, R.J., Ellison, C.A., Knaak, J.B., Ma, C., Olson, J.R., 2011. Cytochrome
560 P450-specific human PBPK/PD models for the organophosphorus pesticides:
561 Chlorpyrifos and parathion. *Toxicology* 285, 57–66. doi:10.1016/j.tox.2011.04.002
- 562 Fukumitsu, H., Ohtsuka, M., Murai, R., Nakamura, H., Itoh, K., Furukawa, S., 2006.
563 Brain-Derived Neurotrophic Factor Participates in Determination of Neuronal
564 Lamina Fate in the Developing Mouse Cerebral Cortex. *J. Neurosci.* 26, 13218–
565 13230. doi:10.1523/JNEUROSCI.4251-06.2006

- 566Gatzeva-topalova, P.Z., Warner, L.R., Pardi, A., Carlos, M., 2011. NIH Public Access
567 18, 1492–1501. doi:10.1016/j.str.2010.08.012.Structure
- 568Gillespie, L.N., Clark, G.M., Bartlett, P.F., Marzella, P.L., 2003. BDNF-induced
569 survival of auditory neurons in vivo: Cessation of treatment leads to accelerated
570 loss of survival effects. *J. Neurosci. Res.* 71, 785–790. doi:10.1002/jnr.10542
- 571Gim, J., Kim, H.S., Kim, J., Choi, M., Kim, J.R., Chung, Y.J., Cho, K.H., 2010. A
572 system-level investigation into the cellular toxic response mechanism mediated by
573 AhR signal transduction pathway. *Bioinformatics* 26, 2169–2175.
574 doi:10.1093/bioinformatics/btq400
- 575Gohlke, J.M., Griffith, W.C., Faustman, E.M., 2005. A systems-based computational
576 model for dose-response comparisons of two mode of action hypotheses for
577 ethanol-induced neurodevelopmental toxicity. *Toxicol. Sci.* 86, 470–484.
578 doi:10.1093/toxsci/kfi209
- 579Goudarzi, H., Nakajima, S., Ikeno, T., Sasaki, S., Kobayashi, S., Miyashita, C., Ito, S.,
580 Araki, A., Nakazawa, H., Kishi, R., 2016. Prenatal exposure to perfluorinated
581 chemicals and neurodevelopment in early infancy: The Hokkaido Study. *Sci. Total*
582 *Environ.* 541, 1002–1010. doi:10.1016/j.scitotenv.2015.10.017
- 583Haley, B., Zamore, P.D., 2004. Kinetic analysis of the RNAi enzyme complex. *Nat.*
584 *Struct. Mol. Biol.* 11, 599–606. doi:10.1038/nsmb780
- 585Hood, L., Heath, J.R., Phelps, M.E., Lin, B., 2004. Systems biology and new
586 technologies enable predictive and preventative medicine. *Science* 306, 640–643.
587 doi:10.1126/science.1104635
- 588Johansson, N., Fredriksson, A., Eriksson, P., 2008. Neonatal exposure to
589 perfluorooctane sulfonate (PFOS) and perfluorooctanoic acid (PFOA) causes
590 neurobehavioural defects in adult mice. *Neurotoxicology* 29, 160–169.
591 doi:10.1016/j.neuro.2007.10.008
- 592Kell, D.B., 2006. Systems biology, metabolic modelling and metabolomics in drug
593 discovery and development. *Drug Discov. Today* 11, 1085–1092.
594 doi:10.1016/j.drudis.2006.10.004
- 595Kitano, H., 2002. Systems biology: A brief overview. *Sci. (New York, NY)* 295, 1662–
596 1664. doi:10.1126/science.1069492
- 597Kohler, J.J., Schepartz, A., 2001. Kinetic Studies of Fos , Jun , DNA Complex
598 Formation : DNA Binding Prior to Dimerization. *Biochemistry* 40, 130–142.
599 doi:10.1021/bi001881p
- 600Li, W., He, Q.Z., Wu, C.Q., Pan, X.Y., Wang, J., Tan, Y., Shan, X.Y., Zeng, H.C.,
601 2015. PFOS Disturbs BDNF-ERK-CREB Signalling in Association with Increased
602 MicroRNA-22 in SH-SY5Y Cells. *Biomed Res. Int.* 2015.
603 doi:10.1155/2015/302653
- 604Lipsky, R.H., Marini, A.M., 2007. Brain-derived neurotrophic factor in neuronal
605 survival and behavior-related plasticity. *Ann. N. Y. Acad. Sci.* 1122, 130–143.
606 doi:10.1196/annals.1403.009

- 607 Long, Y., Wang, Y., Ji, G., Yan, L., Hu, F., Gu, A., 2013. Neurotoxicity of
608 Perfluorooctane Sulfonate to Hippocampal Cells in Adult Mice. *PLoS One* 8, 1–9.
609 doi:10.1371/journal.pone.0054176
- 610 Louisse, J., Beekmann, K., Rietjens, I.M.C.M., 2016. Use of physiologically based
611 kinetic modeling-based reverse dosimetry to predict in vivo toxicity from in vitro
612 data. *Chem. Res. Toxicol.* *acs.chemrestox.6b00302*.
613 doi:10.1021/acs.chemrestox.6b00302
- 614 Lu, B., 2003. Pro-Region of Neurotrophins. *Neuron* 39, 735–738. doi:10.1016/S0896-
615 6273(03)00538-5
- 616 Lubin, F.D., Roth, T.L., Sweatt, J.D., 2008. Epigenetic regulation of BDNF gene
617 transcription in the consolidation of fear memory. *J. Neurosci.* 28, 10576–86.
618 doi:10.1523/JNEUROSCI.1786-08.2008
- 619 Ma, E., MacRae, I.J., Kirsch, J.F., Doudna, J.A., 2008. Autoinhibition of Human Dicer
620 by Its Internal Helicase Domain. *J. Mol. Biol.* 380, 237–243.
621 doi:10.1016/j.jmb.2008.05.005
- 622 Menei, P., Montero-Menei, C., Whittemore, S.R., Bunge, R.P., Bunge, M.B., 1998.
623 Schwann cells genetically modified to secrete human BDNF promote enhanced
624 axonal regrowth across transected adult rat spinal cord. *Eur. J. Neurosci.* 10, 607–
625 621. doi:10.1046/j.1460-9568.1998.00071.x
- 626 Michael, G.J., Averill, S., Nitkunan, A., Rattray, M., Bennett, D.L., Yan, Q., Priestley,
627 J. V., 1997. Nerve growth factor treatment increases brain-derived neurotrophic
628 factor selectively in TrkA-expressing dorsal root ganglion cells and in their central
629 terminations within the spinal cord. *J. Neurosci.* 17, 8476–90.
- 630 Mowla, S.J., Pareek, S., Farhadi, H.F., Petrecca, K., Fawcett, J.P., Seidah, N.G., Morris,
631 S.J., Sossin, W.S., Murphy, R. a, 1999. Differential sorting of nerve growth factor
632 and brain-derived neurotrophic factor in hippocampal neurons. *J. Neurosci.* 19,
633 2069–2080.
- 634 Muiños-Gimeno, M., Espinosa-Parrilla, Y., Guidi, M., Kagerbauer, B., Sipilä, T.,
635 Maron, E., Pettai, K., Kananen, L., Navinés, R., Martín-Santos, R., Gratacòs, M.,
636 Metspalu, A., Hovatta, I., Estivill, X., 2011. Human microRNAs miR-22, miR-
637 138-2, miR-148a, and miR-488 are associated with panic disorder and regulate
638 several anxiety candidate genes and related pathways. *Biol. Psychiatry* 69, 526–
639 533. doi:10.1016/j.biopsych.2010.10.010
- 640 Murer, M., Yan, Q., Raisman-Vozari, R., 2001. Brain-derived neurotrophic factor in
641 the control human brain, and in Alzheimer's disease and Parkinson's disease. *Prog.*
642 *Neurobiol.* 63, 71–124. doi:10.1016/S0301-0082(00)00014-9
- 643 O'Leary, P.D., Hughes, R.A., 1998. Structure-activity relationships of conformationally
644 constrained peptide analogues of loop 2 of brain-derived neurotrophic factor. *J.*
645 *Neurochem.* 70, 1712–21. doi:10.1046/j.1471-4159.1998.70041712.x
- 646 Pérez-Ortín, J.E., Alepuz, P.M., Moreno, J., 2007. Genomics and gene transcription
647 kinetics in yeast. *Trends Genet.* 23, 250–257. doi:10.1016/j.tig.2007.03.006
- 648 Perruisseau-Carrier, C., Jurga, M., Forraz, N., McGuckin, C.P., 2011. MiRNAs stem

- 649 cell reprogramming for neuronal induction and differentiation. *Mol. Neurobiol.* 43,
650 215–227. doi:10.1007/s12035-011-8179-z
- 651Rodríguez-Tébar, A., Dechant, G., Götz, R., Barde, Y.A., 1992. Binding of
652 neurotrophin-3 to its neuronal receptors and interactions with nerve growth factor
653 and brain-derived neurotrophic factor. *EMBO J.* 11, 917–922.
- 654Sandhya, V.K., Raju, R., Verma, R., Advani, J., Sharma, R., Radhakrishnan, A.,
655 Nanjappa, V., Narayana, J., Somani, B.L., Mukherjee, K.K., Pandey, A.,
656 Christopher, R., Keshava Prasad, T.S., 2013. A network map of BDNF/TRKB and
657 BDNF/p75NTR signaling system. *J. Cell Commun. Signal.* 7, 301–307.
658 doi:10.1007/s12079-013-0200-z
- 659Sato, I., Kawamoto, K., Nishikawa, Y., Tsuda, S., Yoshida, M., Yaegashi, K., Saito, N.,
660 Liu, W., Jin, Y., 2009. Neurotoxicity of perfluorooctane sulfonate (PFOS) in rats
661 and mice after single oral exposure. *J. Toxicol. Sci.* 34, 569–574.
662 doi:10.2131/jts.34.569
- 663Thiel, C., Cordes, H., Conde, I., Castell, J.V., Blank, L.M., Kuepfer, L., 2017. Model-
664 based contextualization of in vitro toxicity data quantitatively predicts in vivo drug
665 response in patients. *Arch. Toxicol.* 91, 865–883. doi:10.1007/s00204-016-1723-x
- 666Timchalk, C., Nolan, R.J., Mendrala, A.L., Dittenber, D.A., Brzak, K.A., Mattsson, J.L.,
667 2002. A physiologically based pharmacokinetic and pharmacodynamic (PBPK/PD)
668 model for the organophosphate insecticide chlorpyrifos in rats and humans.
669 *Toxicol. Sci.* 66, 34–53. doi:10.1093/toxsci/66.1.34
- 670Vuong, A.M., Yolton, K., Webster, G.M., Sjödin, A., Calafat, A.M., Braun, J.M.,
671 Dietrich, K.N., Lanphear, B.P., Chen, A., 2016. Prenatal polybrominated diphenyl
672 ether and perfluoroalkyl substance exposures and executive function in school-age
673 children. *Environ. Res.* 147, 556–564. doi:10.1016/j.envres.2016.01.008
- 674Wambaugh, J.F., Setzer, R.W., Pitruzzello, A.M., Liu, J., Reif, D.M., Kleinstreuer,
675 N.C., Wang, N.C.Y., Sipes, N., Martin, M., Das, K., DeWitt, J.C., Strynar, M.,
676 Judson, R., Houck, K.A., Lau, C., 2013. Dosimetric anchoring of In vivo and In
677 vitro studies for perfluorooctanoate and perfluorooctanesulfonate. *Toxicol. Sci.*
678 136, 308–327. doi:10.1093/toxsci/kft204
- 679Wang, X., Li, Y., Xu, X., Wang, Y. hua, 2010. Toward a system-level understanding of
680 microRNA pathway via mathematical modeling. *BioSystems* 100, 31–38.
681 doi:10.1016/j.biosystems.2009.12.005
- 682Waters, M.D., Boorman, G., Bushel, P., Cunningham, M., Irwin, R., Merrick, A.,
683 Olden, K., Paules, R., Selkirk, J., Stasiewicz, S., Weis, B., Van Houten, B.,
684 Walker, N., Tennant, R., 2003. Systems toxicology and the Chemical Effects in
685 Biological Systems (CEBS) knowledge base. *Environ. Health Perspect.* 111, 811–
686 824. doi:10.1289/txg.5971
- 687Yang, J., Wang, C., Nie, X., Shi, S., Xiao, J., Ma, X., Dong, X., Zhang, Y., Han, J., Li,
688 T., Mao, J., Liu, X., Zhao, J., Wu, Q., 2015. Perfluorooctane sulfonate mediates
689 microglial activation and secretion of TNF- α through Ca²⁺-dependent PKC-NF-
690 κ B signaling. *Int. Immunopharmacol.* 28, 52–60. doi:10.1016/j.intimp.2015.05.019

691 York, N., 2015. Regulation of Cell Survival by Secreted Proneurotrophins.pdf. Science
692 (80-.). 294, 1945–1949. doi:10.1126/science.1065057

693 You, H.J., Park, J.H., Pareja-Galeano, H., Lucia, A., Shin, J. Il, 2016. Targeting
694 MicroRNAs Involved in the BDNF Signaling Impairment in Neurodegenerative
695 Diseases. NeuroMolecular Med. doi:10.1007/s12017-016-8407-9

696 Yu, N., Wei, S., Li, M., Yang, J., Li, K., Jin, L., Xie, Y., Giesy, J.P., Zhang, X., Yu, H.,
697 2016. Effects of Perfluorooctanoic Acid on Metabolic Profiles in Brain and Liver
698 of Mouse Revealed by a High-throughput Targeted Metabolomics Approach. Sci.
699 Rep. 6, 23963. doi:10.1038/srep23963

700 Zeng, H. cai, Zhang, L., Li, Y. yuan, Wang, Y. jian, Xia, W., Lin, Y., Wei, J., Xu, S.
701 qing, 2011. Inflammation-like glial response in rat brain induced by prenatal PFOS
702 exposure. Neurotoxicology 32, 130–139. doi:10.1016/j.neuro.2010.10.001

703 Zhang, L., Li, Y.-Y., Zeng, H.-C., Wei, J., Wan, Y.-J., Chen, J., Xu, S.-Q., 2011.
704 MicroRNA expression changes during zebrafish development induced by
705 perfluorooctane sulfonate. J. Appl. Toxicol. 31, 210–222. doi:10.1002/jat.1583

706 Zhao, Y., Ricci, P.F., 2010. Modeling dose-response at low dose: A systems biology
707 approach for ionization radiation. Dose-Response 8, 456–477. doi:10.2203/dose-
708 response.09-054.Zhao

709

710

711

712

713Figure Labels

714Figure 1. describes the miRNA-mRNA-BDNF-cell survival mechanistic pathway
715showing the importance of miRNA in regulating BDNF via forming a complex with
716RNA-induced silencing complex. Later BDNF binding to TrkB with the sequential
717activation of pathway **such as MAPK/ERK and PI3K/AKT causing increase in**
718**CREB expression which leads to increase in** neuronal survival, differentiation, and
719proliferation.

720Figure 2. represents the full scheme of PBPK/PD model showing the integration of
721tissue dosimetry model with miRNA-BDNF-Cell survival pathway via
722pharmacodynamic interaction of PFOS-miRNA.

723Figure 3. Schema for the estimation of in-vivo oral dose

724Figure 5. Simulated brain concentrations of PFOS over the time period. The figure
725shows a simulation of the time course of PFOS concentration in the brain for each 12
726different doses corresponding to in-vitro dose. The single oral dose was given at 240hr.

727Figure 4. represents the pharmacodynamic interaction of PFOS-miRNA and the
728consequent effect on neuronal survivability rate.

729Figure 6. Mechanistic Base model. The figure shows simulated key biomolecules such
730as RISC, miRNA, RISCm, BDNF and percentage neuronal cell survivability.

731Figure 7. simulated time vs miRNA level The figure depicts simulated miRNA
732concentration after single oral dose of PFOS for 12 different dose levels.

733Figure 8. Simulated time vs RISCm level. The figure shows the increase in RISCm
734level after single oral dose of PFOS for 12 different dose levels.

735Figure 9. Simulated time vs BDNF level. The figure depicts simulated BDNF
736concentration after single oral dose of PFOS for 12 different dose levels.

737Figure 10. Simulated vs predicted neuronal cell survivability (percentage). The figure
738depicts simulated vs observed neuronal cell survivability (percentage) after single oral
739dose of PFOS for 12 different dose levels.

740

741 TABLES

742 Table 1. oral equivalent dose calculated based on AUC extrapolation method

in-vitro dose (μM)	AUC_24 (nM*hr)	AUC_48 (nM*hr)	in-vivo dose (nM)(24hr)	in-vivo dose (nM) (48hr)
1	24000	48000	86925	130570
10	240000	480000	896550	1362850
50	1200000	2400000	4494910	6839718
100	2400000	4800000	8992868	13685810
150	3600000	7200000	13490820	20531899
200	4800000	9600000	17988780	27378025

743

744 Table 2. Scaled parameters for Coupled PBPK/PD mechanistic pathway model

Description	Parameter Symbol	Value	References
BDNF synthesis rate	K _{in_BDNF}	.023 nM/hr/kg 0.75	(Menei et al., 1998)
BDNF dissipation rate	K _{out_BDNF}	0.231/hr	(Fukumitsu et al., 2006)
Maximum BDNF effect on cell survival	E _{max}	100	Assumed
Half maximum concentration of BDNF for neuron survivability	EC _{50_BDNF}	5E-03 nM	(O'Leary and Hughes, 1998)
Cell degradation constant	K _{d_cell}	2.45e-5/hr	(Clarke et al., 2000)
Maximum PFOS effect on miRNA	E _{max_miRNA}	2.4	maximum fold change(Li et al., 2015)
Half maximum stimulatory concentration of PFOS for miRNA	EC _{50_PFOS}	1000nM	(Li et al., 2015)
Volume of cytoplasm	V _{cyt}	4e-12/L	(Bartlett and Davis, 2006)
Volume of nucleus	V _{nucleus}	4e-13	(Carlotti et al., 2000)
Pri miRNA synthesis rate	K _{primiRNA}	3.6 nM/hr	(Pérez-Ortín et al., 2007)
mRNA synthesis rate	K _{mRNA}	0.36 nM/hr	(Bartlett and Davis, 2006)
Adjusted Coefficient of R promoting pri-miRNA maturation	R _{miRNA}	0.001 nM	(Wang et al., 2010)

pri-miRNA to pre-miRNA(n) catalyzed by R	K_primiRNA-premiRNA	360/hr	(Wang et al., 2010)
premiRNA transport rate	T_premiRNA	180/hr	(Wang et al., 2010)
Rate of premiRNA(c) conversion to dsRNA	K_premiRNA-dsRNA	36/hr	(Ma et al., 2008)
miRNA formation rate	K_miRNA	36/hr	(Kohler and Schepartz, 2001)
miRNA-induced RISC formation rate	K_RISC	108/hr	(Bartlett and Davis, 2006)
mRNA-RISC complex formation rate	K_[mRNA-RISC]	3.6nM/hr	(Haley and Zamore, 2004)
mRNA cleavage rate	Kc_mRNA	25.27	(Haley and Zamore, 2004)
Dissociation rate of RISC complex	Kd_[mRNA-RISC]	3.6/hr	(Wang et al., 2010)
Rate of pri-miRNA degradation	d_primiRNA	0.9/hr	(Wang et al., 2010)
Rate of pre-miRNA(c) degradation	d_premiRNA	0.9/hr	(Wang et al., 2010)
Rate of dsRNA degradation	d_dsRNA	3.96/hr	(Wang et al., 2010)
Rate of miRNA degradation	d_miRNA	0.9/hr	(Wang et al., 2010)
Rate of RISC degradation	d_RISC	0.36/hr	(Wang et al., 2010)
Rate of mRNA-bound RISC complex degradation	d_[mRNA-RISC]	0.077/hr	(Wang et al., 2010)
Rate of mRNA degradation	d_mRNA	0.36/hr	(Wang et al., 2010)

745